ELSEVIER

Thermochimica Acta 255 (1995) 143–154

thermochimica acta

Thermal decomposition of barium and strontium peroxides

Michael J. Tribelhorn, Michael E. Brown *

Chemistry Department, Rhodes University, Grahamstown 6140, South Africa

Received 26 July 1994; accepted 13 October 1994

Abstract

Isothermal TG studies of the thermal decompositions in nitrogen of barium (490–610°C) and strontium (380–530°C) peroxides to the corresponding oxides with the evolution of gaseous oxygen showed that reactions were deceleratory overall with an initial relatively rapid process followed by the main deceleratory reaction. Curves of fractional decomposition (α) against time could be described by the Ginstling–Brounshtein diffusion model (low α) and the first-order rate equation (BaO_2, $\alpha > 3.0$; SrO_2, $\alpha > 0.5$). The activation energy for the main deceleratory process of the decomposition of BaO_2 is 185 ± 5 kJ mol^{-1}, which is considerably higher than the value of 119 ± 2 kJ mol^{-1} for the deceleratory stage of the SrO_2 decomposition. Non-isothermal kinetic analyses gave similar E_a values for the decompositions of both BaO_2 and SrO_2, namely 165 ± 5 kJ mol^{-1}. Possible mechanisms are discussed.

Keywords: Barium peroxide; Decomposition; Isothermal; Mechanism; Strontium peroxide; TG

1. Introduction

Several studies of the decomposition of the alkaline-earth peroxides have been reported [1–26]. However, only a few of these studies report values for the kinetic parameters. No kinetic parameters for the decomposition of SrO_2 were found in the literature.

* Corresponding author.

SSDI 0040-6031(94)02156-2

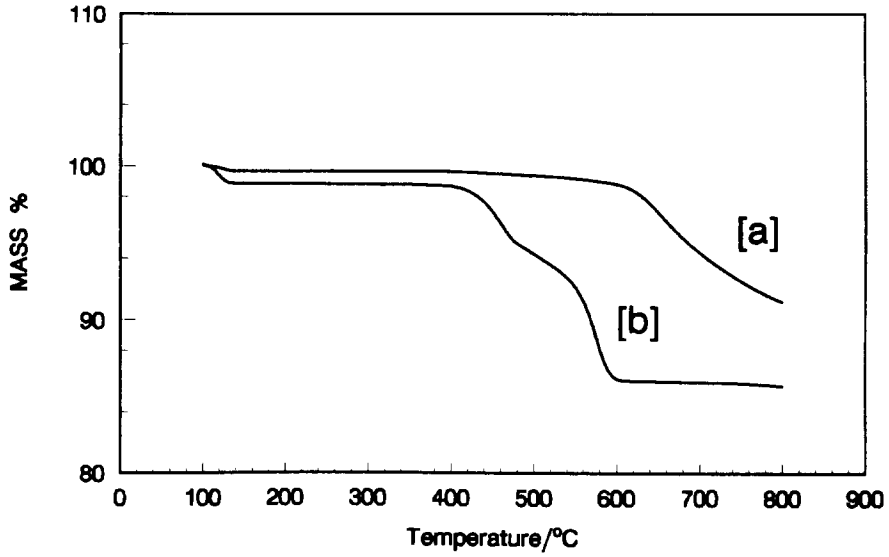

Fig. 1. TG of BaO_2 [a] and SrO_2 [b] heated at 20°C min^{-1} in N_2.

DSC traces for BaO_2 samples heated in N_2 showed a high-temperature endotherm (>600°C) attributed to the decomposition of BaO_2 [1]. The expected enthalpy change, calculated from standard enthalpies of formation, was 56.5 kJ mol^{-1}. The measured value of 64.7 kJ mol^{-1} for 85% pure BaO_2 (which is corrected to 76.2 kJ mol^{-1} for 100% BaO_2) compared well with the 80.1 kJ mol^{-1} recorded by Till [2]. Drennan and Brown [1] also reported an endotherm at 360°C, which they ascribed to the dehydroxylation of $Ba(OH)_2$, present as an impurity in some of the samples studied. The high-temperature decomposition endotherm recorded in nitrogen was absent in the traces for all samples heated in O_2 up to the instrument limit of 725°C, indicating that decomposition is shifted to higher temperatures in the presence of O_2.

TG curves for BaO_2 heated in N_2 at 20°C min^{-1} (Fig. 1, curve [a]) showed the removal of small amounts ($\approx$0.2%) of moisture at $\approx$100°C, the onset of decomposition above 500°C and the maximum rate at $\approx$680°C. The 7.7% mass loss found agrees well with the expected loss of 8.0% for decomposition of 85% pure BaO_2 to BaO and O_2. In O_2, onset of decomposition was shifted to $\approx$700°C and the maximum rate to $\approx$730°C.

DSC studies [1] of the behaviour of SrO_2 in N_2 showed two endotherms with onset temperatures at 390°C (400°C in O_2) and 525°C (550°C in O_2), corresponding to ΔH values of 23.1 $\pm$ 6.7 and 15.9 $\pm$ 3.9 kJ mol^{-1}. The total ΔH value for the two endotherms recorded is 43.9 kJ mol^{-1}, which converts to 51.7 kJ mol^{-1} for 100% purity. Fahim and Ford [3] recorded a value of 48.1 kJ mol^{-1}. The endotherms were smaller in O_2 (11.7 $\pm$ 3.6 and 15.3 $\pm$ 1.2 kJ mol^{-1}, respectively), due to the inhibition of decomposition by the O_2 atmosphere. As the sample mass was increased and less rapid flushing was used, the first endotherm increased in intensity

until the second endotherm virtually disappeared. This endotherm was often preceded by a small exotherm, associated with the dehydroxylation of $Sr(OH)_2$.

The TG curve for SrO_2 in N_2 (Fig. 1, curve [b]) shows that, after the initial loss of adsorbed water ($<1\%$) at 100°C, decomposition occurs in two steps: the first with mass loss $\approx 4.0\%$ and onset at 390°C, is followed by loss of a further $\approx 8.0\%$, onset at 525°C (calculated 11.4% for decomposition of 85% pure SrO_2 to SrO and O_2). This value of $\approx 12.0\%$ coincides well with previous studies [1] which recorded a value of 12.7%. A further gradual loss of $\approx 2.0\%$ occurs toward the limit of the instrument at 900°C (decomposition of some $SrCO_3$). In O_2, the relative mass losses in the two stages (8–9% followed by 3–4%) and the onset temperatures are dependent on the pressure of O_2. The DTG curve of the decomposition agrees well with DSC curves of SrO_2 in N_2.

The isothermal decomposition of BaO_2 has been reported [3] to obey first-order kinetics, with an activation energy E_a of 135 kJ mol^{-1}. The non-isothermal decomposition was also studied [3] and the value of E_a, determined from a plot of $\ln(\ln(1-\alpha))/T^2$ versus $1/T$, was 141 kJ mol^{-1}. Although the kinetics deviated strongly from first-order behaviour above 800°C, this was explained in terms of diffusion resistance.

Erofeev and Sokolova [4] obtained a value of $E_a = 192$ kJ mol^{-1} for the isothermal decomposition of BaO_2 (based on $\alpha = 1 - \exp(-kt^n)$). Mayorova et al. [5] used programmed temperature thermogravimetry and obtained a value for E_a of 360 ± 20 kJ mol^{-1} by assuming first-order behaviour. Brunere and Dokuchaeva [6] represented the decomposition of BaO_2 by a three-step process: nucleus formation ($E_a = 12$ kJ mol^{-1}); grain growth ($E_a = 104$ kJ mol^{-1}); and oxygen diffusion ($E_a = 2$ kJ mol^{-1}). The details of this research were not available.

2. Experimental

2.1. Materials

The materials used in this study were: BaO_2, Unilab Saarchem, <20 μm, 85% pure, main impurity BaO; SrO_2, Bernardy Chemie, <20 μm, 85% pure, main impurity SrO.

2.2. Thermal analysis apparatus

Perkin-Elmer Delta series TGA7 and DSC7 instruments were used. The TG furnace was calibrated magnetically using the Curie points of nickel (354°C) and iron (780°C). Unless otherwise stated, the TG was continuously flushed with nitrogen flowing at 6 cm^3 min^{-1}. The sample pans used in the TG were platinum.

DSC experiments were performed in Al pans (below 575°C) and in Pt pans (below 725°C). The DSC was calibrated using the melting temperatures of pure ($>99.9\%$) indium (onset 156.60°C) and zinc (onset 419.45°C), and the peak area was calibrated using the enthalpy of fusion of indium (28.45 J g^{-1}). N_2 was used as the purge gas (flow rate 50 cm^3 min^{-1}).

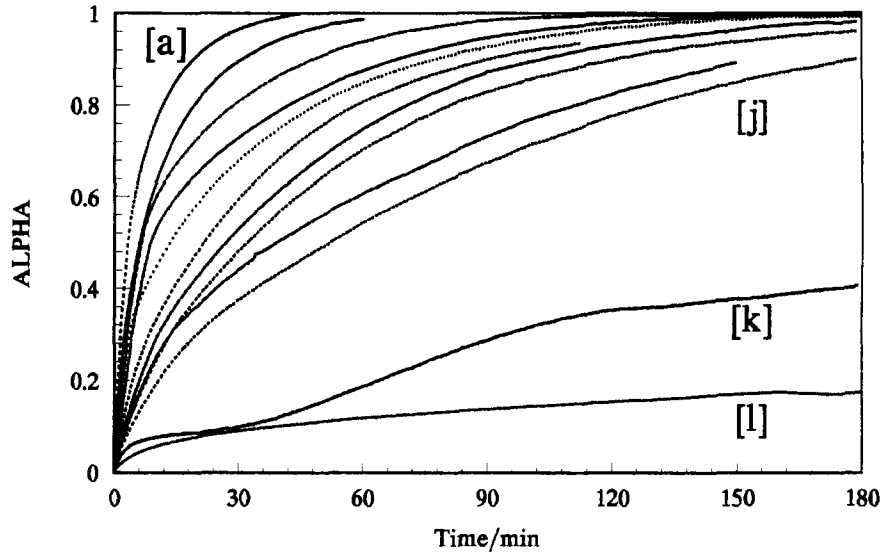

Fig. 2. Isothermal decomposition of BaO_2 in N_2: [a] 610; [b] 600; [c] 590; [d] 570; [e] 550; [f] 530; [g] 520; [h] 510; [i] 505; [j] 500; [k] 495; and [l] 490°C.

3. Results and discussion

Isothermal TG studies were performed on the peroxide systems at a series of different temperatures (490–610°C for BaO_2 and 380–530°C for SrO_2). The TG curves were converted to α, time curves (where the fractional decomposition, $\alpha = (m_0 - m)/(m_0 - m_f)$ and m_0 and m_f are the initial and final sample masses, respectively). The value of m_f used was that calculated for complete decomposition to the oxide. The isothermal α,t curves at different temperatures are shown in Fig. 2 (BaO_2) and Fig. 3 (SrO_2).

3.1. Decomposition of BaO_2

Decomposition of BaO_2 in N_2, which begins between 490 and 495°C, is very slow at temperatures below 500°C, and reaction does not approach completion. The low-temperature (495°C) curve for the decomposition of BaO_2 (curve [k]) shows at least four stages: (i) an initial deceleratory process ($0 < \alpha < 0.1$); (ii) an approximately linear process ($0.1 < \alpha < 0.25$); (iii) a second deceleratory process ($0.25 < \alpha < 0.3$); and (iv) a very slow approximately linear process which hardly contributes significantly at this temperature, so that the total extent of reaction at low temperatures is only 40% of that expected. Increasing the temperature to 500°C has a marked effect on all of these processes. Processes (i), (ii) and (iii) become almost linear and the final process (iv) shows up as deceleratory.

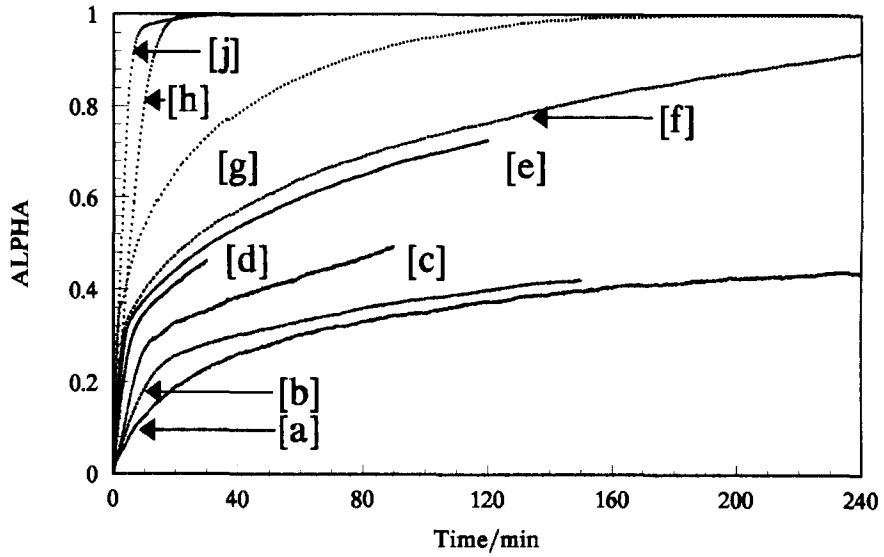

Fig. 3. Isothermal decomposition of SrO_2 in N_2: [a] 380; [b] 390; [c] 400; [d] 420; [e] 430; [f] 440; [g] 480; [h] 520; and [j] 530°C.

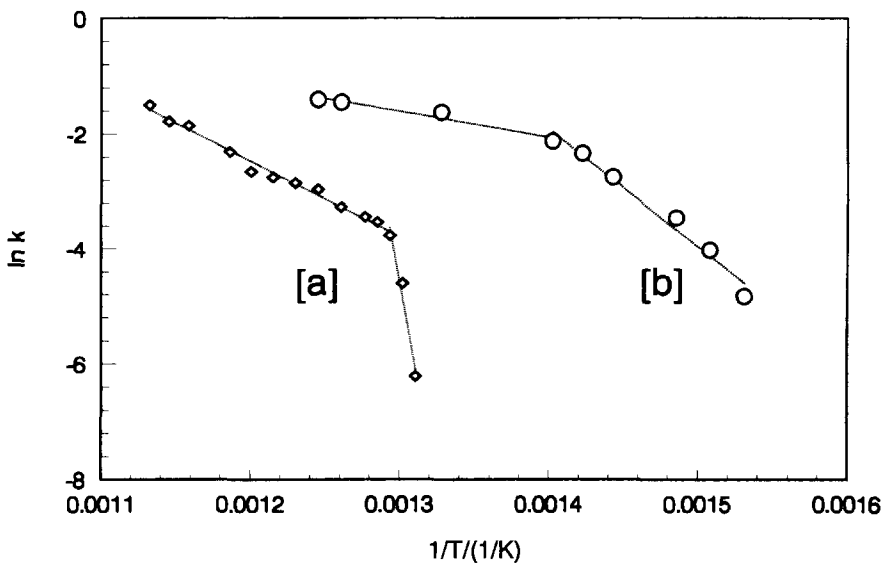

Fig. 4. Arrhenius plots for BaO_2 [a] and SrO_2 [b].

As an approximate kinetic analysis of the first stages of reaction, the initial slopes s_0 of the α,t curves were measured and $\ln s_0$ was plotted against $1/T$ (Fig. 4, curve [a]). This assumes that the initial reaction may be treated as a zero-order reaction; $d\alpha/dt = k = s_0$ (constant over $0 < \alpha < 0.2$). In general, for a rate equation of the

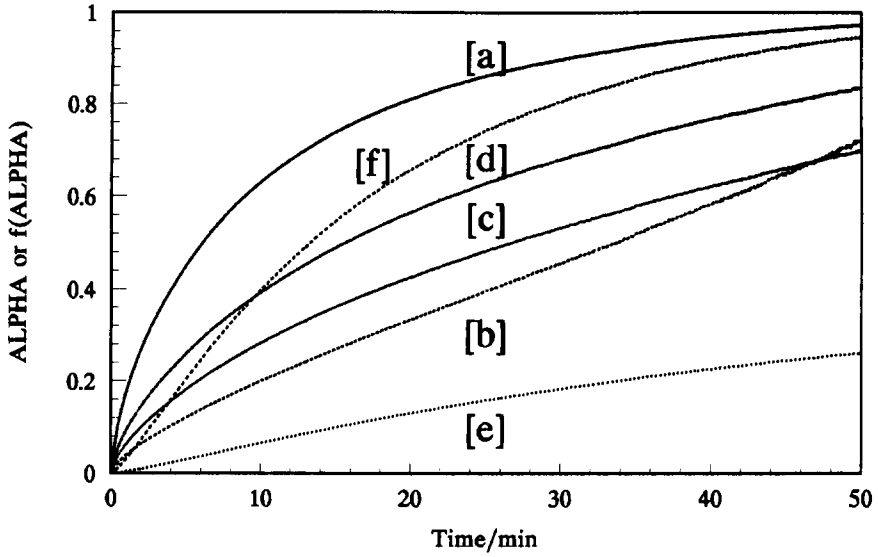

Fig. 5. Test of kinetic models for the isothermal decomposition of BaO_2 at 600°C: [a] α; [b] F1 × 5; [c] R3; [d] R2; [e] D4; and [f] D1.

form $d\alpha/dt = k(1-\alpha)^n$, for $\alpha \ll 1$, $d\alpha/dt \approx k$, and the influence of the apparent order n is removed. Such a treatment gave Arrhenius plots (Fig. 4) with two approximately linear regions. For BaO_2, the change in behaviour occurred at about 770 K (496°C) and the E_a values were 109.4 ± 3.8 kJ mol^{-1} for the higher temperature region and a very high apparent value of ≈ 1200 kJ mol^{-1} for the lower temperatures.

Kinetic analysis of the full α,t curves in terms of the integrated rate equations ($f(\alpha) = k(t - t_0)$) for the standard deceleratory kinetic models [27] is illustrated by the plots in Fig. 5 of $f(\alpha)$ (scaled where necessary for easier comparison) against t. The best description of the experimental results was in terms of either the first-order model (F1) ($f(\alpha) = -\ln(1-\alpha) = k(t - t_0)$) or the Ginstling–Brounshtein diffusion model (D4) ($f(\alpha) = (1 - (2\alpha/3)) - (1-\alpha)^{(2/3)} = k(t - t_0)$) where t_0 is a time correction if the model does not apply from $t = 0$. The α range 0.1–0.8 was used for calculation of k values, but the fit of the F1 and D4 models extended to $\alpha \approx 0.95$. The fit of these models to the data is shown in Figs. 6 and 7 for the F1 and D4 models, respectively. In calculating the fit of the D4 model, it is convenient to calculate $t = f'(\alpha)$ rather than $\alpha = f(t)$. The D4 model shows good agreement with the experimental data from very low values of α until α exceeds about 0.8. The fit of the first-order model to the data is satisfactory only at values of α above 0.3.

The Arrhenius parameters for the BaO_2 decomposition, calculated from the temperature dependence of the above rate coefficients, are listed in Table 1.

The applicability of individual deceleratory models is always difficult to determine, especially when the final stages of reactions are slow and the values of m_f are of limited accuracy. However, the values of E_a determined are not greatly altered by

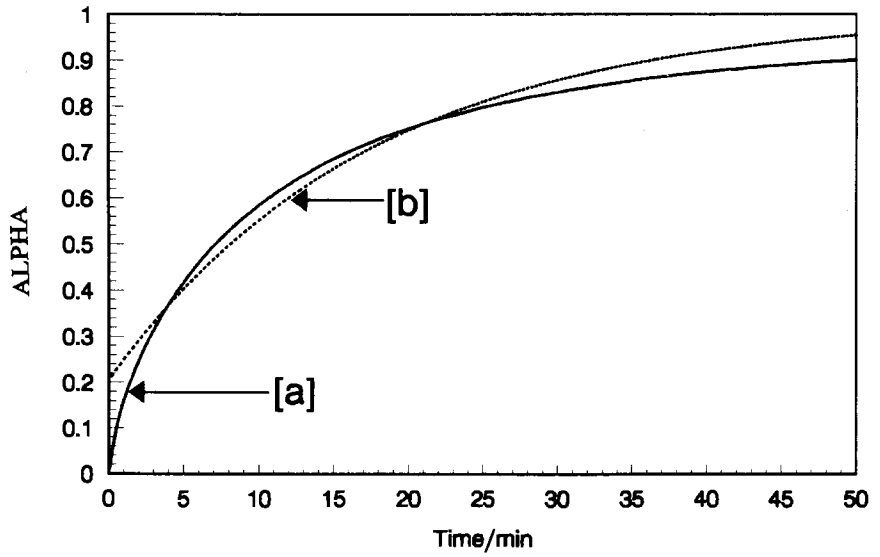

Fig. 6. Fit of the F1 model for the isothermal decomposition of BaO_2 (600°C): [a] experimental; [b] F1 model.

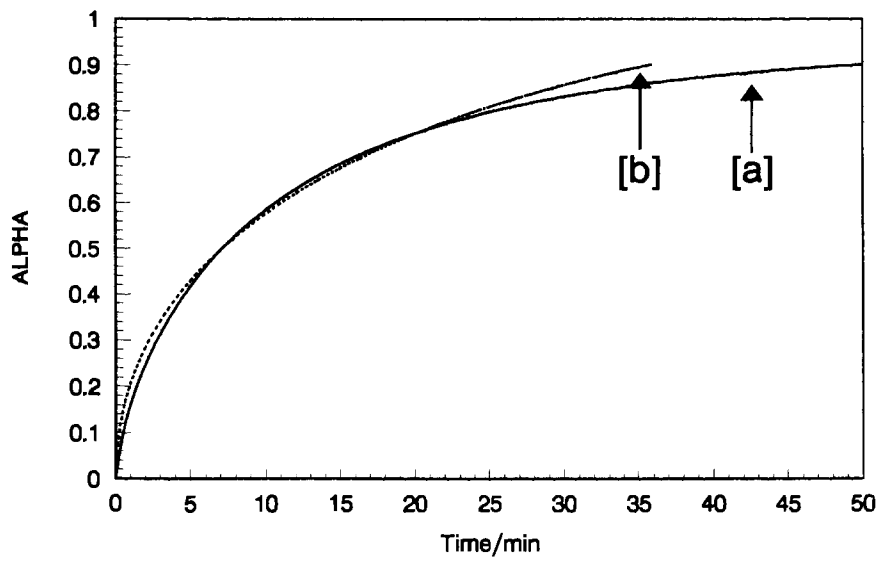

Fig. 7. Fit of the D4 model for the isothermal decomposition of BaO_2 (600°C): [a] experimental; [b] D4 model.

the choice of kinetic model. The value of E_a obtained, 180 ± 3 kJ mol^{-1}, is close to that of 192 kJ mol^{-1} reported by Erofeev [4], but higher than some of the other values reported. The value of E_a for the initial rate process (109.4 ± 3.8 kJ mol^{-1}) is consistent with the findings of Brunere and Dukuchaeva [6] for grain growth.

Table 1
Kinetic parameters for the thermal decomposition of barium and strontium peroxides

Kinetic model		α Range	E_a/(kJ mol^{-1})	A/min^{-1}
Isothermal TG on BaO_2 (560–600°C)				
F1	First order ($n = 1$)	0.1–0.8	182.8 ± 2.6	(42.3 ± 1.1) × 10^9
D4	Ginstling–Brounshtein	0.1–0.8	177.9 ± 1.6	(22.6 ± 0.2) × 10^7
Isothermal TG on SrO_2 (380–390°C)				
D4	Ginstling–Brounshtein	0–0.4	249.6 ± 3.0	(68.8 ± 0.1) × 10^{15}
Isothermal TG on SrO_2 (440–480°C)				
F1	First order ($n = 1$)	0.1–0.9	119.7 ± 0.8	(5.10 ± 0.03) × 10^6
D4	Ginstling–Brounshtein	0.1–0.9	119.3 ± 0.6	(4.42 ± 0.02) × 10^5

System	Order	E_a/(kJ mol^{-1})	A/s^{-1}	r^2 [a]
Non-isothermal kinetics				
BaO_2	$\frac{1}{2}$	160.0 ± 1.2	(92.0 ± 0.3) × 10^7	0.99
	$\frac{2}{3}$	164.5 ± 1.3	(18.4 ± 0.1) × 10^8	0.99
	1	173.5 ± 1.5	(74.0 ± 0.3) × 10^8	0.99
SrO_2	$\frac{1}{2}$	161.8 ± 2.2	(60.0 ± 0.1) × 10^9	0.99
	$\frac{2}{3}$	164.3 ± 2.2	(93.5 ± 0.1) × 10^9	0.99
	1	169.4 ± 2.1	(22.7 ± 0.1) × 10^{10}	0.99

[a] Correlation coefficient.

Variations in kinetic parameters are to be expected on account of the reversible nature of the decomposition. The conditions used in the above experiments, namely small sample masses and rapid removal of oxygen product by flushing with nitrogen, would tend to decrease any influence of the reverse reaction. Rate control by removal of oxygen by diffusion is consistent with the D4 model which applies over the major portion of the reaction. Deviation from this model at high values of α could be explained in terms of some recrystallisation of product oxide at the surface slowing reaction more than predicted.

3.2. Decomposition of SrO_2

The isothermal decomposition of SrO_2 (380–530°C) is qualitatively similar to that described above for BaO_2 although the multiple stages at low temperatures are not as clearly defined (Fig. 3, curve [a]). The marked effect of temperature on the initial stages results in these stages becoming so rapid that initial mass losses at higher temperatures are approximately linear. The increase in rate of the final deceleratory stage, with consequent increase in extent of decomposition within a fixed time, is shown in Fig. 3.

The Arrhenius plot is shown in Fig. 4, curve [b]. The activation energy for the initial stages, determined, as for BaO_2, from the initial slopes, showed a distinctive

change in slope at about 440°C. The value of E_a determined for the lower temperature range was 170 ± 14 kJ mol^{-1}, and that of the higher temperature range a much lower 37.2 ± 6.2 kJ mol^{-1}. These values are both considerably smaller than the values obtained for BaO_2. The low value of E_a at high temperatures suggests diffusion control.

The kinetic models used in the analysis of the BaO_2 results were also applied to the overall α,t curves for the decomposition of SrO_2. The low temperature (380°C) behaviour is best described by the D4 model, while the F1 and D4 models provide the best description of the kinetic behaviour at the higher temperatures (480°C), as was found for BaO_2. The agreement between these models (predicted values) and the experimental data at 480°C is shown in Figs. 8 and 9. The Ginstling–Brounshtein model agrees well with the data at values of α up to 0.8 (Fig. 9), as it did for the BaO_2 decomposition. The agreement between the first-order model and the experimental data is reasonable above α values of 0.5 (Fig. 8).

At the lower temperatures (380–390°C) the overall extent of reaction is decreased to about 40% of the expected total in more than four hours. These deceleratory curves could also be fitted approximately by the D4 model for $0.1 < \alpha < 0.4$. The apparent activation energy for this temperature region (Table 1) was 250 ± 3 kJ mol^{-1} which is higher than the other values estimated. The practical consequence of a high activation energy is the sensitivity to temperature displayed. TG studies support the indications that two different mechanisms occur during decomposition of the peroxide. This would account for the fitting of different models to the initial and the later stages of the decomposition curve.

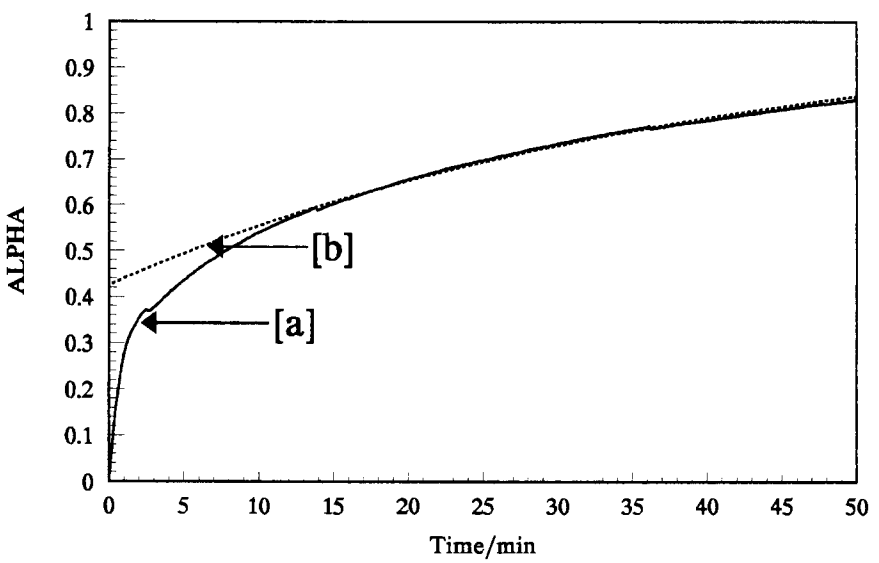

Fig. 8. Fit of the F1 model for the isothermal decomposition of SrO_2 (480°C): [a] experimental; [b] F1 model.

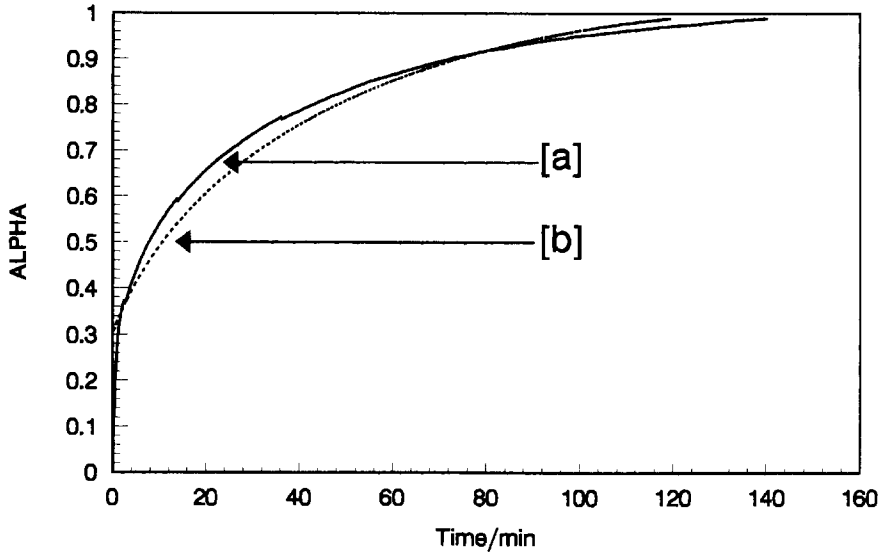

Fig. 9. Fit of the D4 model for the isothermal decomposition of SrO_2 (480°C): [a] experimental; [b] D4 model.

3.3. Non-isothermal kinetic analysis

The Borchardt and Daniels method [28] was used to obtain kinetic parameters from programmed temperature thermal analysis studies. The TG curves (in N_2 at 20 K min^{-1}) were converted to α,T curves and plots of α against $1/T$ and of $\ln[(d\alpha/dt)/(1-\alpha)^n]$ against $1/T$ for various values of n were examined for linearity. The Arrhenius parameters calculated from the slopes and intercepts of the appropriate linear regions of the plots are listed in Table 1. The apparent activation energies for the two peroxides are similar and not very different from the values obtained for BaO_2 from isothermal experiments. The non-isothermal value of SrO_2 lies between the isothermal values for the low and high temperature experiments. Values of E_a do not depend strongly on the value of n in the range $n = 0.5-1.0$. Since the mechanism of decomposition of BaO_2 becomes relatively complex beyond $\alpha \approx 0.6$, determination of kinetic data was restricted to this range. Similarly for the SrO_2, the complex behaviour beyond $\alpha \approx 0.4$ (being a combination of the two decomposition stages, superimposed upon one another) restricts determination of the kinetic data for the initial decomposition to the region $0 < \alpha < 0.4$.

4. Conclusions

The isothermal decompositions of both of the peroxides, BaO_2 and SrO_2, are deceleratory overall with an initial relatively rapid process followed by the main deceleratory reaction. At temperatures where decomposition to the oxide is com-

plete, the initial process appears as an apparently linear region ($0 < \alpha < 0.2$) and the temperature dependences of these linear regions give rise to apparent activation energies of ≈ 1200 kJ mol^{-1} at low temperatures (onset of decomposition) and 109.4 ± 3.8 kJ mol^{-1} at higher temperatures for BaO_2; and corresponding values of 169.5 ± 13.5 and 37.2 ± 6.2 kJ mol^{-1} for low and high temperature behaviour, respectively, of SrO_2.

The main deceleratory process is best described by the diffusion-based Ginstling–Brounshtein model (D4). The activation energy for this stage of the decomposition of BaO_2 is 185 ± 5 kJ mol^{-1}, which is considerably higher than the value of 119 ± 2 kJ mol^{-1} for the deceleratory stage of the SrO_2 decomposition. The value of 185 ± 5 kJ mol^{-1} for the decomposition of BaO_2 is in good agreement with the value of 192 kJ mol^{-1} reported by Erofeev and Sokolova [4], but higher than that reported by Fahim and Ford [3] of 135 kJ mol^{-1}.

The non-isothermal kinetic analyses gave similar E_a values for the decompositions of both BaO_2 and SrO_2 of 165 ± 5 kJ mol^{-1}. The value for BaO_2 lies between the values mentioned above and this may be as a result of the averaging effect of the programmed temperature measurements. Apparent activation energies were considerably greater than the corresponding overall enthalpies of decomposition quoted above in the Introduction.

It is clear from the above studies of the two peroxides that their thermal decomposition is far from the simple process represented by

$$MO_2(s) \rightarrow MO(s) + 0.5O_2(g)$$

The reversibility is well established, i.e.

$$MO_2(s) \rightleftharpoons MO(s) + 0.5O_2(g)$$

but under the conditions applying in this study, i.e. rapid removal of product gas from small sample masses, the reverse reaction is unlikely to be very significant.

One of the ways of accounting for different decomposition mechanisms for apparently chemically uniform material over one temperature range, is to suggest different reactivities of portions of the sample, determined by differing degrees of imperfection of these portions. Many examples of such behaviour have been reported, for example $KMnO_4$, NH_4ClO_4, etc. [27], and Brunere [6] has suggested that decomposition occurs by the three-step process of nucleus formation, grain growth and oxygen diffusion, with initiation of decomposition occurring at imperfections.

When different mechanisms operate over different temperature ranges, either a chemical or a physical explanation may be put forward. A chemical explanation would require the occurrence of different bonding situations within the sample, e.g. dehydration of $CuSO_4 \cdot 5H_2O$. The MO_2 crystal structure is tetragonal (*I4/mmm*) and it is possible that the energy requirements for loss of oxygen via the steps

$$O_2^{2-} \rightarrow O^{2-} + O$$

$$2O \rightarrow O_2(g)$$

may be different for different sets of O_2^{2-} ions in the peroxide structure. This aspect is being studied theoretically [29]. The third, and perhaps most likely, explanation for changes of mechanism could be the influence of some recrystallisation of the product oxide on the course of reaction, i.e.

$$MO_2(c) \rightarrow MO(a) + 0.5O_2(g)$$

and

$$MO(a) \rightarrow MO(c)$$

where c is crystalline and a is amorphous. Such processes have been suggested in the dehydration of hydrates and in many decompositions, especially those of alkaline-earth carbonates. The rate of removal of oxygen from the peroxide by diffusion could be drastically altered by the formation of a crystalline layer of oxide on the surface where O_2 gas is eventually to be released.

References

[1] R.L. Drennan and M.E. Brown, Thermochim. Acta, 208 (1992) 201, 223, 247.
[2] L. Till, J. Therm. Anal., 3 (1971) 177.
[3] M.A. Fahim and J.D. Ford, J. Chem. Eng., 27 (1983) 21.
[4] B.J. Erofeev and N.D. Sokolova, Topokinetic Equation Tables, Akad. Nauk BSSR, Minsk, (1963) 3.
[5] A.F. Mayorova, S.N. Mudretsova, M.N. Mamontov, P.A. Levashov and A.D. Rusin, Thermochim. Acta, 217 (1993) 241.
[6] V.J. Bruenere and A.N. Dokuchaeva, Izv. Akad. Nauk Latvijskoj SSR, Ser. Chim., 3 (1990) 332.
[7] V.D. Hogan and S. Gordon, J. Phys. Chem., 61 (1957) 1401.
[8] S. Nakahara and T. Hikita, J. Ind. Exp. Soc. Jpn., 21 (1960) 2.
[9] S. Nakahara, J. Ind. Exp. Soc. Jpn., 22 (1961) 259.
[10] V. Averbuh and G. Chufarov, Zh. Obsthei Khim., 21 (1951) 626.
[11] S. Makarov and M. Grigorieva, Isv. Akad. Nauk USSR, 7 (1959) 1168.
[12] M. Tzentnershver and M. Blumenthal, Bull. Inorg. Acad. Pol., Ser. A, (1935) 540.
[13] Y. Azuma, M. Mizuide and K. Suehiro, Gyp. Lim., 162 (1979) 175.
[14] S. Tamaru and K. Shiomi, Z. Phys. Chem., A171 (1935) 221.
[15] S. Tamaru and K. Shiomi, Z. Phys. Chem., A171 (1935) 229.
[16] V. Dolgov and A. Basharin, Vestn. Akad. Nauk SSSR, 2 (1978) 10.
[17] J.A. Hedvall, Z. Anorg. Allg. Chem., 104 (1918) 163.
[18] M. Blumenthal, Rocz. Chem., 13 (1933) 5.
[19] M. Blumenthal, J. Chem. Phys., 31 (1934) 489.
[20] V. Osika, V. Annopolskii and V. Karpenko, Tr. NIPI Osnov. Khim., 51 (1979) 17.
[21] Y. Pelovsky, V. Raynova, I. Gruncharov and I. Dombalov, J. Therm. Anal., 37 (1991) 841.
[22] I.I. Volnov, Dokl. Akad. Nauk SSSR, 94 (1954) 477.
[23] I.I. Volnov, Zh. Neorg. Khim., 3 (1958) 402.
[24] H.G. Wiedemann and G. Bayer, Proc. 1st Eurp. Symp. on Therm. Anal., (1976) 295.
[25] M.E. Brown and R.L. Drennan, 14th Int. Pyrotech. Sem., (1989) 423.
[26] J.A. Hedvall and N. Zweigbergk, Z. Anorg. Allg. Chem., 108 (1919) 119.
[27] M.E. Brown, D. Dollimore and A.K. Galwey, Comprehensive Chemical Kinetics, Vol. 22, Reactions in the Solid State, Elsevier, Amsterdam, 1980.
[28] H.J. Borchardt and F. Daniels, J. Am. Chem. Soc., 79 (1957) 41.
[29] A. de La Croix, MSc Thesis, Rhodes University, in preparation.